J Mater Sci (2007) 42:6279–6286
DOI 10.1007/s10853-006-1242-x

Photoconductivity of n-type semiconductor nanoparticle-doped poly(N-vinylcarbazole) films

Tadahiro Murakata Aita · Kosuke Iha · Liu Hui · Takeshi Higuchi · Shimio Sato

Received: 8 November 2005 / Accepted: 10 November 2006 / Published online: 21 April 2007

Abstract TiO_2, CdS and ZnS nanoparticles that disperse stably in organic solvents are synthesized. Poly(N-vinylcarbazole) films doped with the n-type semiconductor nanoparticles are prepared with a cast method. The films exhibit a transient photocurrent when irradiated by a light pulse and act such as a diode when AC voltage is applied under continuous illumination. The transient photocurrent response and diode-like properties are significantly different depending on the kind of the nanoparticles and their amounts. The films doped with TiO_2 and CdS nanoparticles increase the transient photocurrent at lower doped amounts, which is remarkable for TiO_2-doped films. Time of flight analysis of the transient photocurrent shows that mobility of hole in PVK increases with increase in the amount of CdS and TiO_2. From the studies on the diode-like properties, the current increase at lower dopant concentration is concluded to be due to increase in the amount of holes by an electron transfer from PVK to the photo-excited nanoparticles. At higher doping with CdS nanoparticles, main charge carrier of the films is found to change from holes to electrons.

Introduction

In recent years, nanoparticles have attracted much attention. Many articles about their preparation, morphology and optical properties have been reported [1]. Among the nanoparticles, much interest has focused on some metal and semiconductor nanoparticles because of their unique optical properties. Nanoparticles of noble metals, such as gold, silver and copper, show intense colors that are quite different from those of their bulk phase. The coloration is caused by surface plasmon absorption of the particles [2]. Semiconductor nanoparticles, such as CdS and CdSe nanoparticles, show another kind of spectral change. Their absorption spectra shift to shorter wavelength [3]. The blue shift is caused by the size quantization effect that increases band gap energy of the semiconductor particles [4].

Besides such unique optical properties, nanoparticles may be attractive as components of various composite materials. Nanoparticles are able to interact strongly with circumference owing to their large surface area. If semiconductor nanoparticles can be dispersed homogeneously in optically or electrically active materials and interacted with them, various enhanced or tuned optical or electrical properties may appear. From the expectation, several workers studied composite materials containing nanoparticles [5, 6]. As an example, study on photoconductivity of poly(N-vinylcarbazole) film doped with CdS nanoparticles was mentioned [7]. Poly(N-vinylcarbazole), hereafter called PVK, is well known as a photoconductive polymer and has been used as a charge transport material in xerographic systems. The polymer is photoconductive because the photo-excitation of its carbazole group generates holes to carry electric charge [8]. The disadvantage of PVK as photoconductive materials is to be low in hole drift mobility and to be insensible to visible light. The doping with CdS nanoparticles was found to enhance the hole mobility [7], although the reasons why such a n-type semiconductor nanoparticle enhance the hole drift mobility have not been clear yet.

T. M. Aita (✉) · K. Iha · L. Hui · T. Higuchi · S. Sato
Department of Materials Science and Engineering, Yamagata University, 4-3-16 Yonezawa, 992-8510 Yamagata, Japan
e-mail: aita@yz.yamagata-u.ac.jp

To prepare high quality nanocomposite materials, nanoparticles have to disperse homogeneously in host materials. However, most nanoparticles are stable only as a solution and, once separated from the solvent, they aggregate and no longer disperse. In the present study, we prepared TiO_2, CdS and ZnS nanoparticles which disperse in organic solvents. PVK film was easily doped with the n-type semiconductor nanoparticles with a cast method. Photoconductive properties of the nanocomposite films are investigated through measurement of their transient photocurrents and diode-like actions.

Experimental

Materials

All the solvents used for the synthesis of nanoparticles and for preparation of polymer films were distilled before use. Other chemicals used for the synthesis of nanoparticles were of reagent grade and used as received. PVK was purchased from Kanto Kagaku. It was used as received because purification by reprecipitation did not affect the photoconductive properties. Commercially available TiO_2 (anatase) and CdS powders were also used as dopants. Polystyrene (PS, degree of polymerization n = 1,600–1,800) was used as a typical non-photoconductive polymer. They were purchased from Wako Chemicals and used as received.

Synthesis of semiconductor nanoparticles and their characterization

TiO_2 nanoparticles were synthesized by the same procedure as reported previously [9]. Briefly, 10 mL of titanium tetraisopropoxides was dissolved in 50 mL of EtOH. To the solution, HCl solution consisting of 1 mL of HCl (36 wt%) and 30 mL of EtOH, and then H_2O–EtOH solution consisting of 1 mL of H_2O and 30 mL of EtOH were added slowly. After standing the solution overnight, 2.93 g of titanate coupling agent, isopropyl tris(dioctyl pyrophosphate) titanate, was added to it. The molar ratio of the coupling agent to Ti was 0.07. The solution was refluxed for 5 h. Then it was evaporated to remove EtOH and HCl. The crude product was pulverized and, to remove excess coupling agent, washed in n-hexane for 5 h under stirring. TiO_2 particles obtained as precipitates were filtrated and dried at room temperature in vacuo for 6 h.

CdS and ZnS nanoparticles which disperse in organic solvents were synthesized using the corresponding nanoparticles and alkyl thiols as follows. First, thioglycerol-modified nanoparticles were synthesized by a method similar to that reported by Vossmeyer et al. [10]. At the synthesis of CdS nanoparticles, 4.41 mmol of cadmium acetate dihydrate, 6.24 mmol of thiourea and 5.48 mmol of 1-thioglycerol as a modifier were dissolved in 100 mL of DMF. The solution was refluxed for 4 h under argon flow. Then 20 ml of H_2O was added to the solution, which was refluxed again for 2 h. To the solution of thioglycerol-modified nanoparticles, 5.48 mmol of 1-dodecanthiol as a secondary modifier was added and refluxed 1 h. During the reflux, CdS particles precipitated. The reaction mixture was centrifuged and the precipitate was collected by filtration. The CdS nanoparticles obtained as precipitates were washed three times with EtOH. They were stored as a wet cake because the complete drying decreased the dispersibility of the nanoparticles. ZnS nanoparticles were synthesized similarly by using zinc acetate dihydrate as a Zn source.

The nanoparticles were characterized by X-ray diffractometry, scanning electron microscope (SEM) or transmission electron microscope (TEM) observation and optical spectrum measurements. The TiO_2 nanoparticles showed no apparent X-ray diffraction peak. Their solution showed an absorption spectrum typical for TiO_2 although slightly shifted to shorter wavelength. Their particle size estimated from SEM observation was below 10 nm. CdS and ZnS nanoparticles showed broad X-ray diffraction peaks which could be assigned to lattice spacings of CdS and ZnS crystal structures, respectively. The crystalline sizes, calculated from half-width of the X-ray peaks by using Scherrer's equation, were ca. 1–2 nm. The band-gap energies calculated from absorption edge of their solution were 3.02 eV for CdS nanoparticles and >4.0 for ZnS nanoparticles. At ZnS nanoparticles, no accurate value could be obtained because of the disturbance from solvent's absorption. The energies were greater than those of bulk crystals owing to size quantization effect: the values of bulk CdS and ZnS crystals are 2.6 and 3.7 eV, respectivity [11]. The particle sizes of commercial CdS and ZnS particles were determined by SEM observation. Their sizes were distributed from submicrometers to about 20 μm and the larger particles were lumps of smaller particles of less than a few micrometers.

Preparation of polymer films

PVK of 0.2 g and the nanoparticles of required amount were dissolved in 4 mL of THF-benzene mixture (1/1 of THF/benzen by volume). The solution was dropped on a glass plate electrode coated with transparent indium tin oxide (ITO) and spread with a mechanically sliding blade. The polymer solution was dried at room temperature and the resultant film was annealed at 50 °C for 1 h. After the annealing, a circular Au electrode of 0.64 cm^2 was

deposited on the film by a vacuum vapor deposition method. Similar polymer films were also prepared using the commercial semiconductor particles and PS. After photoconductivity measurements, the polymer films were torn from the ITO glass and their thickness was measured with an electromagnet thickness meter. The thickness of the polymer films ranged between 3.5 μm and 5.5 μm.

Photoconductivity measurement

Figure 1 shows the apparatus used for transient photocurrent measurements. A DC voltage was applied to the sample and, at several hundred milliseconds after the voltage application, ITO side of the sample was irradiated with a light pulse from a Xe flash lamp. The electric power applied to the lamp was 0.3 J and half-width of the light pulse was 3 μs. Transient photocurrent from the sample was converted to a voltage signal through a resistor R (=10 kΩ). The signal was amplified 100 times with a wide band amplifier and recorded on a digital oscilloscope. The signal was collected several tens of times and averaged to increase S/N ratio. The resolution time of the system, calculated from the capacitance of the sample and the resistance of R, was a few microseconds, which has the same order of magnitude as the light pulse duration. Mobility μ of charge carriers in the films was determined by the time of flight (TOF) analysis which employs the following equation [12]

$$\mu = L^2/t_\tau V \tag{1}$$

where L is a film thickness, V a voltage applied to the film and t_τ the time at which a flexural point appears in a decay of transient photocurrent. The t_τ relates to the time required for the charge carriers to drift across the film.

Figure 2a shows a circuit used for the investigation of diode-like action of the films, and Fig. 2b illustrates the mechanism of the diode-like action of the film. Continuous illumination to the film generates charge carriers at a location close to the ITO electrode. If photo-generated holes act as charge carriers (p-type conduction), they drift to the Au electrode when the ITO electrode is positively charged, and a photocurrent flows from the ITO electrode to the Au. On the other hand, if photo-generated electrons act as charge carriers (n-type conduction), they drift when ITO is negatively charged and photocurrent flows to the reverse direction. Thus, when AC voltage is applied, it is rectified and DC current flows. The direction of the DC current flow represents the kind of charge carrier and its magnitude is proportional to the amount of the charge carriers. At the measurements, 50 Hz of AC voltage was applied to the sample illuminated constantly with a 500 W Hg lamp. The output current was composed of DC current resulting from the rectification and AC current passing through the sample owing to the capacitance arising from sandwich structure of the sample. The AC current was blocked by choke coil L_1 and L_2 (15H), and bypassed by C_1 (10 μF) whereas the DC current passed through L_1 and L_2 and was charged in C_2 (10 μF). The polarity and voltage at C_2 were measured with a micro-voltmeter. To confirm the rectification of AC voltage applied, the waveform at C_1 was monitored with a digital oscilloscope.

All the measurements were carried out at room temperature.

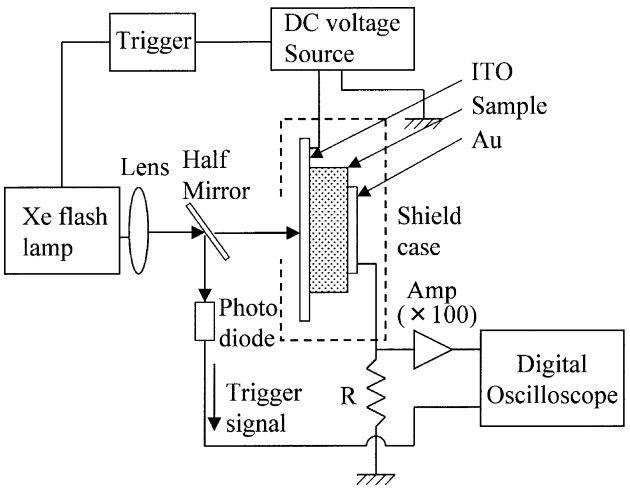

Fig. 1 Schematic diagram of the experimental setup for the measurement of transient photocurrent

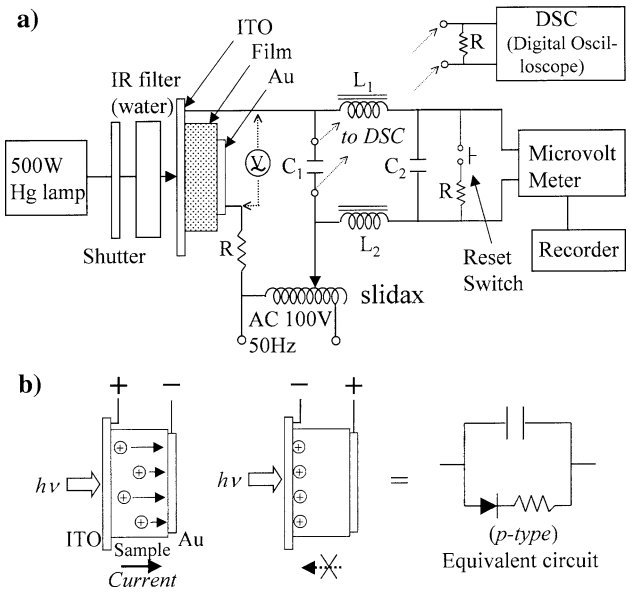

Fig. 2 Electric circuit used for the measurement of diode-like action of films (**a**) and schematic diagram of charge carrier drift in films at p-type conduction (**b**)

Results

All the PVK and PS films doped with the nanoparticles were transparent but the polymer films doped with commercial particles were opaque. Figure 3 shows the typical transient photocurrents for PVK, PVK doped with CdS nanoparticles (here after called CdS/PVK) and PS doped with CdS nanoparticles (CdS/PS) films. The inset shows the transient photocurrent for PVK film doped with commercial CdS particles (Com-CdS/PVK). The CdS/PVK and CdS/PS films contained 5wt% of the nanoparticles and the Com-CdS/PVK film 1.25 wt% of the commercial particles. In all measurements, the ITO electrode (irradiated side) was positively charged. The transient photocurrent for the PVK film showed a slow decay of which duration was a few milliseconds. The decay was similar to that reported by other workers [7].

The transient photocurrent for Com-CdS/PVK film was quite different from those for PVK and CdS/PVK films: Com-CdS/PVK film showed a very fast decay while PVK and CdS/PVK films showed slow ones. From the fact that the charge carriers (electrons) in a bulk CdS crystal have high mobility, we thought that the transient photocurrent for the Com-CdS/PVK was caused mainly by drift of electrons in the photo-excited CdS particles. To confirm this, t_τ values were calculated by adopting typical experimental conditions, i.e. an applied voltage V of 50 V, a film thickness L of 5 μm and a CdS particle size of 4 μm, and μ values of 340 cm^2/Vs published for CdS [13] and of 1×10^{-6} cm^2/Vs published for PVK [14]. The values calculated from 1 were 5 ms for the PVK film and 10 ps for the CdS particles. The one calculated for the PVK film almost agreed with the duration of the decay for PVK film. On the other hand, the value calculated for the Com-CdS particles was far smaller than the duration of the decay for the Com-CdS/PVK film. In such a very fast relaxation system, the transient photocurrent flows only in the duration of a light pulse and the resulting waveform is prolonged depending on the resolution time of the measurement system. The duration of the decay of the Com-CdS/PVK film almost agreed with that of the light pulse. Thus the transient photocurrent was caused by drift of the electrons in the photo-excited commercial CdS particles.

In contrast to the Com-CdS/PVK film, CdS/PVK film showed a slow decay and its duration was almost the same as that of the PVK film. This suggests that, in CdS/PVK film, the transient photocurrent was caused by drift of holes in PVK. The CdS/PS film showed a negligibly small transient photocurrent. Since PS is a non-conductive polymer, a transient photocurrent, if flows in the CdS/PS flim, results only from drift of electrons in CdS nanoparticles. The drift of charge carriers, however, is limited in the extremely small particles, and thus may be allowed only when the nanoparticles form large aggregates or contact each other. The negligibly small transient current of CdS/PS film indicates the absence of such aggregates and contacting. Similar behavior was observed also for TiO_2/PS film.

Figure 4 shows comparison of the transient photocurrent of ZnS/PVK film with that of CdS/PVK film. In the same figure, transient photocurrent of the pure PVK film is shown as a reference. Both the films contained 5 wt% of the dopants, CdS or ZnS nanoparticles. Their doping effects are different in two aspects. One is an influence to photocurrent intensity: the doping with ZnS nanoparticles decreased transient photocurrent whereas the doping with CdS nanoparticles increased it. The other is an influence to the decay profile: the decay of ZnS/PVK film has no flexural point whereas those of PVK and CdS/PVK films are flexural. In general, the flexural decay appears when the charge carriers generated in a sheet-like fashion on the irradiated side of the film drift collectively across the film.

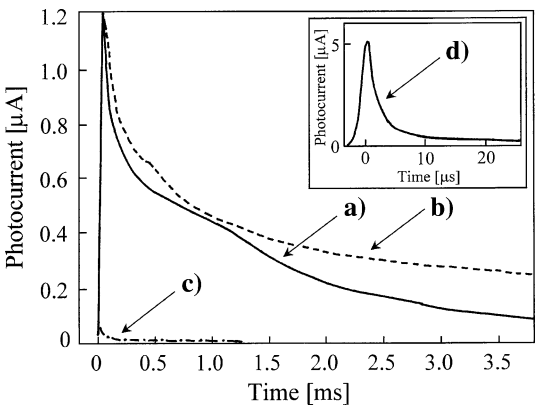

Fig. 3 Transient photocurrent of pure PVK (**a**), CdS/PVK (**b**), CdS/PS (**c**) and Com-CdS/PVK films (**d**) Applied voltage [V/μm]: (**a**) 11.3, (**b**) 12.5, (**c**) 6.6, and (**d**) 3.8

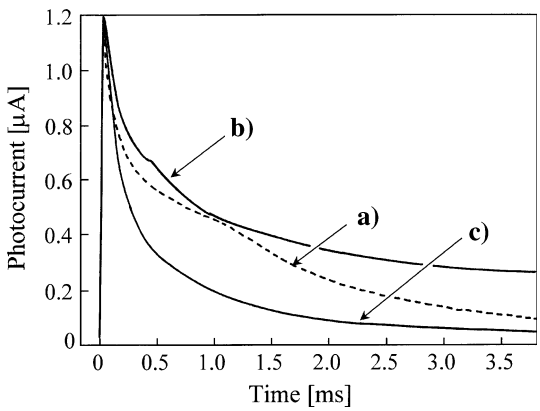

Fig. 4 Transient photocurrent of pure PVK (**a**), CdS/PVK (**b**), ZnS/PVK films (**c**) applied voltage [V/μm]: (**a**) 11.3, (**b**) 12.5, and (**c**) 11.8

In such a case, the mobility of the charge carrier is calculated from the time (t_τ) at which the flexural point appears. The doping with ZnS nanoparticles decreased the transient photocurrent and made the transient photocurrent non-flexural. A similar phenomenon was reported for the case where dopants acted as the trap of a charge carrier or an impurity disturbing the crystallization of the polymer [15]. In this case, no information on the drift of charge carriers is obtained, and therefore the following studies were carried out with CdS/PVK and TiO_2/PVK films.

Figures 5 and 6, respectively, show the transient photocurrents of CdS/PVK and TiO_2/PVK films at various dopant concentrations. The CdS/PVK films showed a flextural point at low dopant concentrations below 15 wt%. The log–log plots of the transient photocurrent I versus time t, shown in the inset, make the flexural points clear. At the low dopant concentrations, the time at which a flexural point appears shortened with increase in the concentration of CdS nanoparticles, as reported by other workers [7]. At higher dopant concentrations above 15 wt%, however, the flexural point disappeared and transient photocurrent decreased. In the case of TiO_2/PVK films, the doping with TiO_2 nanoparticles brought a great increase in transient photocurrent and a flexural point appeared at the low dopant concentrations. At the higher dopant concentrations, the transient photocurrent decreased and the flexural point disappeared as in the case of CdS/PVK films.

Figures 7 and 8 show carrier mobility μ and the number of charge carriers n_c which drifted across the films, respectively. μ was calculated from t_τ by using eq.1 and n_c was calculated by integrating the transient photocurrent from 0 to 3.5 ms. When the transient photocurrent was large, it did not return to zero within 3.5 ms. Therefore n_c was underestimated when the transient photocurrent was large. μ's value obtained for pure PVK is ca. 3×10^{-6} cm^2/Vs, which is somewhat greater than a reported value, ca. 1×10^{-6} cm^2/Vs (at room temperature), although μ is strongly electric field and temperature dependent [14]. The doping with CdS nanoparticles increases μ greatly but the doping with TiO_2 nanoparticles increases it slightly only at a higher dopant concentration. Large difference was found also to n_c value. The doping with CdS nanoparticles increased n_c slightly at 5 wt% but further increase in the dopant concentration decreased it. On the other hand, great increase of n_c occurred in TiO_2/PVK films. n_c's value decreased at higher dopant concentrations above 15wt% but it was still greater than the value of PVK film.

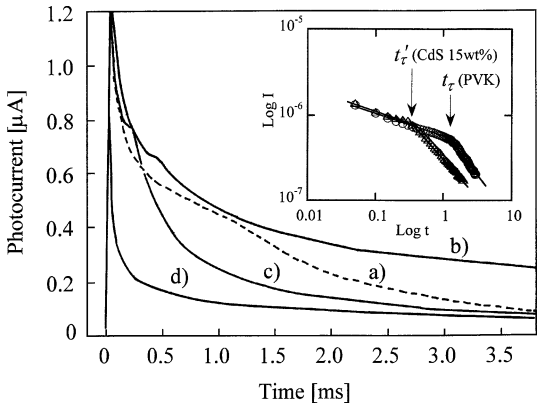

Fig. 5 Transient photocurrent of pure PVK film (**a**) and of CdS/PVK films at dopant concentration of 5 wt% (**b**), 15 wt% (**c**) and 25 wt% (**d**) applied voltage [V/μm]: (**a**) 11.3, (**b**) 12.5, (**c**) 17.1, AND (**d**) 11.5 Inserted figure shows log–log plot of transient photocurrent I versus time t

The doping with CdS and TiO_2 nanoparticles changed μ and n_c of the PVK film. Various causes will be considered. One is the following. The light pulse excited not only PVK but also CdS and TiO_2 nanoparticles, and the photo-excited nanoparticles generated electrons as charge carriers. The mobility of electrons in bulk CdS and TiO_2 crystals are 340 and 4-20 cm^2/Vs, respectively, and far larger than that of holes in PVK. These mobile electrons may participate, in some ways, in the charge drift processes. Thus, to obtain information on the kind and amount of the charge carriers, the diode-like action of the films was investigated.

Figure 9 shows the results for Com-CdS/PS and Com-TiO_2/PS films. The inset shows a waveform of the electric current which went out of the film as it is. The electric current consisted of AC ingredient and DC one. The DC ingredient disappeared without the illumination. This indicates that photo-generated charge carriers caused the diode-like action. The circuit was designed to display positive value when n-type conduction occurred. The positive output signals from the Com-CdS/PS and Com-TiO_2/PS film indicate that the charge carriers of these films are electrons. Since PS is a non-conductive polymer, the electric current should flow only in the n-type semiconductor particles. Therefore the experimental results were rational.

Figure 10 shows the results for CdS/PVK films. The negative output signals from the pure PVK film and the CdS/PVK films at low dopant concentration indicate that holes acted as charge carriers in these films. The intensity of the signal increased by 5 wt% doping with CdS nanoparticles and further doping decreased it. This tendency is consistent well with that of n_c change shown in Fig. 8. These results suggest that, at low dopant concentrations, the photocurrent was caused by drift of holes. At higher doping concentrations of 35 and 50 wt%, however, the output signal changed to positive values, which indicates that the electric conduction changed from p-type conduction to n-type one. This does not conflict with the finding that the transient photocurrent is caused by drift of holes. This is because, when p-type current and n-type one appear

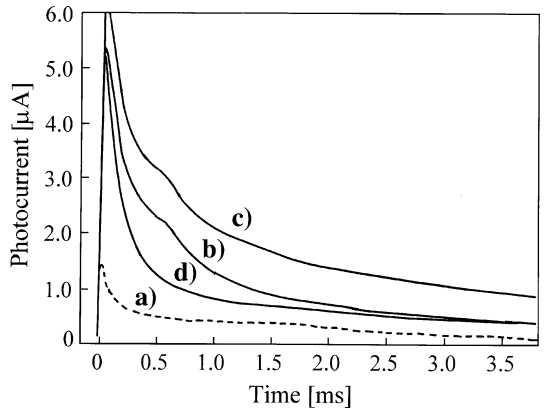

Fig. 6 Transient photocurrent of pure PVK film (**a**) and of TiO_2/PVK films at dopant concentration of 5 wt% (**b**), 15 wt% (**c**) and 35 wt% (**d**) applied voltage [V/μm]: (**a**) 11.3, (**b**) 16.7, (**c**) 17.1, and (**d**) 14.3

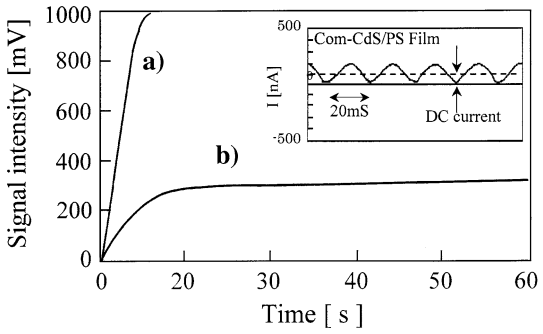

Fig. 9 DC signals generated by diode-like action of Com-TiO_2/PVK film (**a**) and Com-CdS/PVK film Applied AC voltage [V/μm]: (**a**) 1.61, (**b**) 1.33. Inserted figure shows output electric current from Com-CdS/PVK film

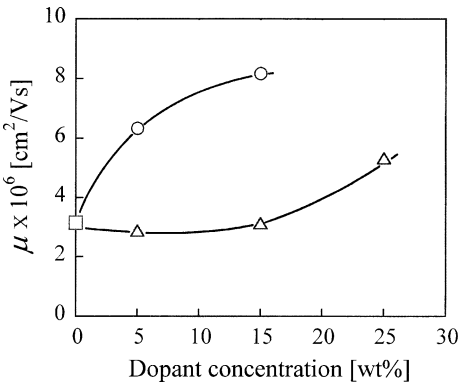

Fig. 7 Effect of dopant concentration on μ of CdS/PVK (○) and TiO_2/PVK films (△)

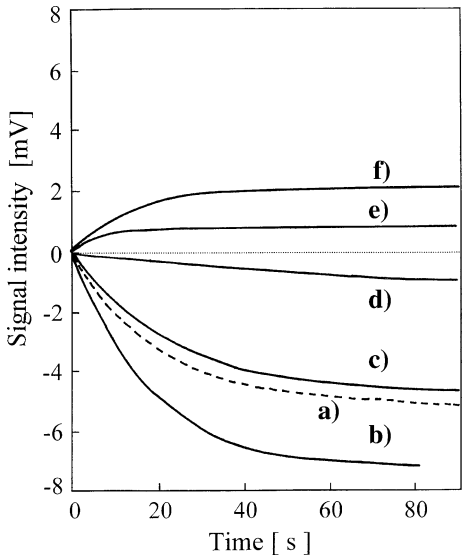

Fig. 10 DC signals generated by diode-like action of pure PVK (**a**) and of CdS/PVK films at dopant concentration of 5 wt% (**b**), 15 wt% (**c**), 25 wt% (**d**), 35 wt% (**e**) and 50 wt% (**f**) applied AC voltage [V/μm]: (**a**) 2.17, (**b**) 2.50, (**c**) 2.27, (**d**) 1.79, (**e**) 2.08, and (**f**) 2.63

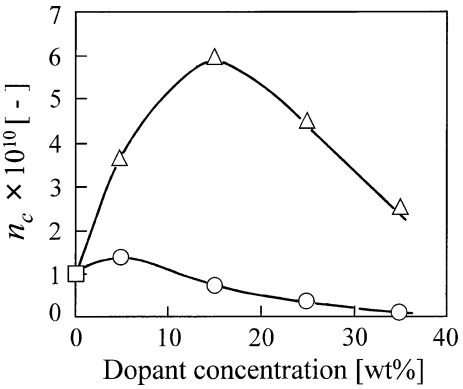

Fig. 8 Effect of dopant concentration on n_c of CdS/PVK (○) and TiO_2/PVK films (△)

by turns, the circuit displays only the difference between the electric currents as an output signal. At the high dopant concentrations, the CdS nanoparticles probably aggregated or contacted each other. Therefore, it is anticipated that n-type conduction along contacting CdS nanoparticles, namely percolation, will occur when ITO electrode is negatively charged whereas p-type conduction will occur in a continuous phase of PVK when the electrode is positively charged.

Figure 11 shows the results for TiO_2/PVK films. All the films showed p-type conduction and the signals were far larger than that of pure PVK film. This indicates that the large increase of the transient photocurrent was caused not by a participation of the electrons but by a great increase of holes. However, the signal intensity started to decrease at 30–50 s after the start of illumination and finally returned to zero. No n-type conduction was observed by further illumination.

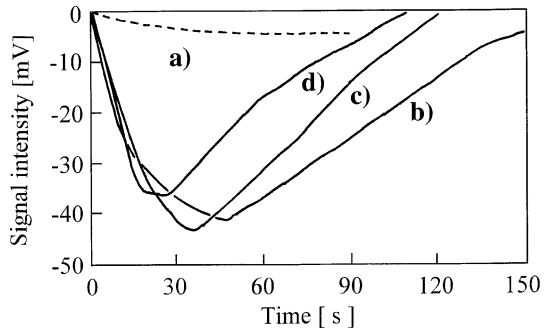

Fig. 11 DC signals generated by diode-like action of pure PVK (**a**) and of TiO_2/PVK films at dopant concentration of 5 wt% (**b**), 15 wt% (**c**), 25 wt% (**d**) applied AC voltage [V/μm]: (**a**) 2.17, (**b**) 2.38, (**c**) 1.92, and (**d**) 2.27

Discussion

By the measurement of the transient photocurrents, several doping effects were revealed. For some of them, we can explain the mechanisms on the basis of results obtained by the measurement of the diode-like actions. Figure 12 shows the possible mechanism for the photocurrent enhancement and related energy diagrams for PVK [16], CdS and TiO_2 [13]. The energy levels shown for CdS and TiO_2 are those for the bulk crystals. Those for the nanoparticles may be a little different from the bulk crystals, especially in the case of CdS nanoparticles, because of size quantization effect. In a PVK film, photo-excitation of carbazole group generates holes, and positive charge is carried by drift of the holes along the neighboring carbazole groups. When PVK is doped with CdS and TiO_2 nanoparticles, the nanoparticles also are excited, and generate electrons and holes on their conduction and valence bands, respectively. The energy levels of the valence band of both the CdS and TiO_2 particles are more positive than highest occupied molecular orbital (HOMO) of the carbazole group, Thus the photo-excited nanoparticles can

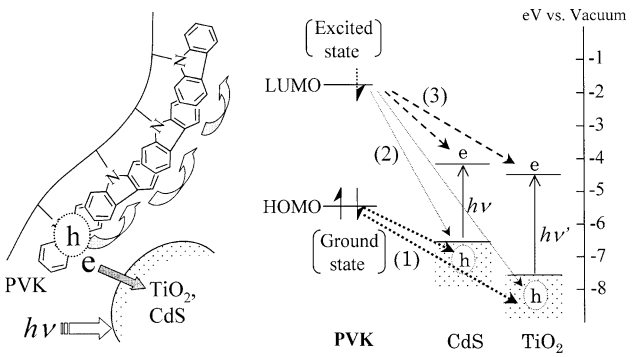

Fig. 12 Energy level diagrams of PVK, CdS and TiO_2, and possible mechanism for electron transfer mechanism which enhance transient photocurrent

abstract an electron from HOMO of a ground state carbazole, as shown by (1), which generates additional holes on the carbazole groups. The photo-excited nanoparticles can abstract an electron also from lowest unoccupied molecular orbital (LUMO) of excited carbazole groups, as shown by (2), but such an opportunity may be a little because the contact between a photo-excited carbazole group and a simultaneously photo-excited nanoparticles is rare. Further, the electrons in LUMO may transfer to the conduction band of the nanoparticles, as shown by (3). The electron-transfer processes shown by (2) and (3) inhibit the recombination of electron–hole pairs in the excited carbazole groups and generate free holes. We speculate that the hole generation is caused mainly by the process (1) rather than (3), because difference, between CdS and TiO_2, in the energy change caused by the process (1) is greater than that by (3). The speculation agrees most with the results obtained for transient photocurrent and n_c values.

The transient photocurrent decreased at higher dopant concentrations. The decrease may be explained in terms of a simple mechanism as follows. The n-type semiconductor nanoparticles act as an insulator to the p-type conduction although the photo-excited nanoparticles enhance the p-type conduction by generating holes in PVK. The higher doping decreases the PVK content and increases the resistance of the film. Further the nanoparticles will scatter the drifting holes and change the drift from collective manner to dispersive one. Thus, at the higher dopant concentrations, the transient photocurrent decreased and the flexural point disappeared.

At the measurement of the diode-like action of TiO_2/PVK films, the signal began to decrease in the middle of the illumination and finally disappeared. Because of the strong oxidation activity, photo-excited TiO_2 nanoparticles not only abstract electrons from carbazole groups to generate holes but also decompose the polymer, especially in the presence of oxygen. The experiments were carried out at the exposure to air and under a strong illumination. This condition will be enough for the polymer to be decomposed. Thus the decrease of the signal would be due to the decomposition of polymer, although detailed mechanism for the decomposition is not clear.

CdS/PVK films showed n-type conduction at higher dopant concentration but TiO_2/PVK films showed only p-type conduction. Two causes are thought about the difference. One relates to the difference in degree of surface modification or structure of the modifier as follows. The modifier of CdS nanoparticles is not so bulky or does not cover the surface so tightly as to disturb the electron transfer between the contacting nanoparticles. In contrast, the modifier of TiO_2 nanoparticles is bulky enough to disturb the electron transfer. Actually, the interactions between the nanoparticles are thought to be different: the

TiO_2 nanoparticles dispersed in various organic solvents whereas the CdS nanoparticles dispersed only in a few organic solvents and no longer dispersed after being dried perfectly. This implies that CdS cores of the CdS nanoparticles interact each other to some extent while the interaction between TiO_2 cores of the TiO_2 nanoparticles is weak. Other workers also pointed out that surface modifiers play an important role in occurrence of electric conductivity of nanoparticles [17]. The other relates to the nature of the inorganic cores of the nanoparticles. CdS nanoparticles showed broad X-ray peaks which can be assigned to CdS crystalline structure while TiO_2 nanoparticles showed no apparent X-ray peak. Thus the cores of the CdS nanoparticles crystallized enough to cause electric conductivity. In contrast, TiO_2 nanoparticles may not have crystallized so fully as to be electrically conductive. At present, it is not clear which of the mechanisms is right.

As for the increase of hole mobility, the mechanism is still unclear. To solve this question, further study is necessary.

Conclusion

We have investigated the photoconductive properties of PVK films doped with semiconductor nanoparticles of CdS, ZnS and TiO_2. The doping of PVK film with ZnS nanoparticles decreased the transient photocurrent. In contrast, when PVK was doped with CdS and TiO_2 nanoparticles, intensity of transient photocurrent and mobility of holes increased at low dopant concentrations. The photocurrent increase was considerable when TiO_2 nanoparticles was used as the dopant. The increase in transient photocurrent was explained in terms of a mechanism that photo-excited nanoparticles abstract electrons from carbazole groups of PVK to generate holes. At higher dopant concentrations, the doping decreased the transient photocurrent and changed the drift from collective manner into dispersive one. Further, in CdS nanoparticle-doped films, percolation of the nanoparticles changed the main electric conduction from p-type conduction to n-type one

References

1. Wang ZL (2000) Characterization of nanophase materials. Wiley-VCH, New York
2. Link S, El-Sayed MA (1999) J Phys Chem B 103:4212
3. Weller H (1993) Angew Chem Int Ed Engl 32:41
4. Brus L (1986) J Phys Chem 90:2555
5. Yuan Y, Fendler JH, Cabasso I (1992) Chem Mater 4:312
6. Schlamp MC, Peng X, Alivisatos AP (1997) J Appl Phys 82:5837
7. Choudhury KR, Samoc M, Patra A, Prasad PN (2004) J Chem Phys B 108:1556
8. Carnes JE, Warter PJ Jr (1972) Phy Rev 5:1557
9. Murakata T, Aita T, Yamamoto R, Yoshida Y, Hinohara M, Ogata T, Stato S (1998) J Chem Eng Jpn 31:21
10. Vossmeyer T, Katsikas L, Giersig M, Popovic IG, Diesner K, Chemseddine A, Eychmuller A, Weller H (1994) J Phys Chem 98:7665
11. Fendler JH (1998) Nanoparticles and nanostructured films. - preparation, characterization and applications. Wiley-VCH, New York, p 450
12. Schein LB, Rosenberg A, Rice SL (1986) J Appl Phys 60:4287
13. Schiavello M (1997) Heterogeneous photocatalysis. Wiley-VCH, New York, pp 8–113
14. Gill WD (1972) J Appl Phys 43:5033
15. Pfister G, Griffiths H (1978) Phys Rev 40:659
16. Yamaguchi M, Nagatomo T (2000) Thin Solid Films 363:21
17. Greenham NC, Peng X, Alivisatos AP (1996) Phys Rev 54:17628